Growth and field-emission property of tungsten oxide nanotip arrays

Jun Zhou, Li Gong, Shao Zhi Deng,[a] Jun Chen, Jun Cong She, and Ning Sheng Xu
National Key Lab of Optoelectronic Materials and Technologies, and Guangdong Province Key Laboratory of Display Material and Technology, School of Physics and Engineering, SunYat-Sen (Zhongshan) University, Guangzhou, 510275, China

Rusen Yang and Zhong Lin Wang[b]
School of Materials Science and Engineering, Georgia Institute of Technology, Atlanta, Georgia 30332-0245

Large-area, quasialigned nanotips of tungsten oxide have been grown by a two-step high-temperature, catalyst-free, physical evaporation deposition process. The tungsten oxide nanotips are single crystalline with growth direction of [010]. The tungsten oxide nanotips exhibit excellent field-emission properties with a low threshold field (for an emission current density of 10 mA/cm^2) ~4.37 MV/m and uniform emission from the entire arrays, as well as high time stability. These results make tungsten oxide nanotip arrays a competitive candidate for field-emission displays. © *2005 American Institute of Physics*. [DOI: 10.1063/1.2136006]

Intensive investigation has been carried out over the last several decades on field emission due to numerous applications such as flat-panel displays, microwave amplifiers, and vacuum microelectronic devices.[1,2] The main requirements for field emitters are low threshold field, high current density, uniform emission, and good stability. To get the low threshold field, the emitters should possess a low work function or surface electron affinity (Φ) or high-field enhancement factor (β), or both. A large number of one-dimensional nanostructures, such as nanotubes,[3–6] nanowires,[7–11] and nanobelts,[12,13] have been considered to be excellent field emission (FE) electron sources emitters because of their high aspect ratio. The needle or tip shape of the nanowire drastically increases the aspect ratio and the field enhancement factor, leading to a reduction in the threshold field.[14–16]

Tungsten oxide is a very important semiconductor. It has been found to be of great applications as an electrochromic device,[17] semiconductor gas sensor,[18] and photocatalyst.[19] Recent research shows that tungsten oxide nanowire/nanorods/nanotubes and nanowire networks have excellent field-emission properties.[20–22] In this paper, we used a two-step growth process to grow quasialigned tungsten oxide nanotip arrays; the nanotips have a needle shape and are well separated from each other; further study shows that they have a uniform and stable field-emission property with a low threshold field.

The tungsten oxide nanotip arrays were prepared by a two-step high-temperature, catalyst-free, physical evaporation deposition process. The experimental setup consists of a vacuum chamber ($\Phi300$ mm$\times 400$ mm), two copper electrodes, a rotary pump system, and a gas controlling system.[9] Tungsten (W) boat (120 mm$\times 20$ mm$\times 0.3$ mm) containing W powders (0.5 g, purity: 99.5%) was placed and fixed on the copper electrodes. Silicon (111) strips were mounted above the boat with their polished surface facing the tungsten boat. After the vacuum chamber was first evacuated down to about ~7.7 Pa, high purity argon gas (99.99%) with a con-

stant flow rate of 200 standard cubic centimeters per minute (sccm) was introduced into the chamber. The evaporation was conducted at ~1400 °C for 10 min and then cooled down and hold at ~1300 °C for another 20 min. During the two-step evaporation process, the temperature of the substrates was ~1072 °C and ~1030 °C, respectively. The prepared products were characterized with high-resolution field-emission scanning electron microscopy (SEM) (Leo 1530 FEG at 10 kV), energy dispersive x-ray spectroscopy (EDS) attached to the SEM, x-ray diffraction (XRD) spectroscopy, and field-emission transmission electron microscopy (TEM) (Hitachi HF-2000 at 200 kV).

Figure 1(a) shows a cross section SEM image of our tungsten oxide nanotip arrays, revealing that large-scale quasialigned nanotips with an average length of ~35 μm were grown on the silicon substrate. An EDS analysis was conducted of the chemical composition of the tungsten oxide nanotips [inset in Fig. 1(a)]. Besides the Si signal coming from the silicon substrate, and the Al signal from the alumi-
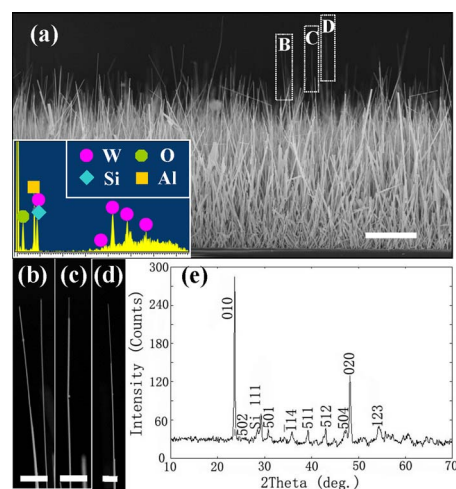

FIG. 1. (a) Low magnification SEM image of tungsten oxide nanotip arrays. Scale bar 10 μm. The inset is the EDS of the tungsten oxide nanotips. (b), (c), and (d) are the enlarged SEM images of the (B), (C), and (D) regions in (a), indicating the tip shape. Scale bar 1 μm. (e) XRD pattern of the tungsten oxide nanotip arrays.

[a]Electronic mail: stsdsz@zsu.edu.cn (SZD)
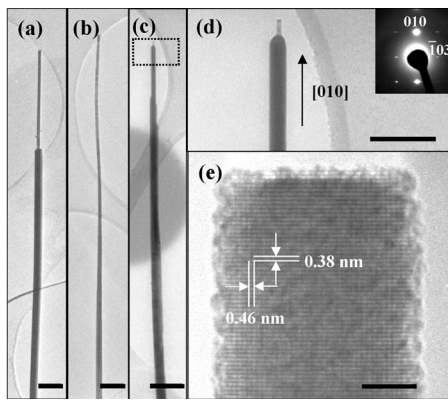[b]Electronic mail: zhong.wang@mse.gatech.edu (ZLW)

FIG. 2. (a), (b) Low magnification TEM images of two different kinds of tungsten oxide nanotips. Scale bar 500 nm. (c) Low magnification TEM image of a segmented tip-on-tip shape tungsten oxide nanotip. Scale bar 500 nm. (d) Enlarged TEM image from the rectangle-enclosed area of (c). Scale bar 250 nm. The inset is the corresponding SAED pattern. (e) High-resolution TEM image of the tungsten oxide nanotip. Scale bar 5 nm.

num SEM holder, only W and O are detected in the nanotips. The higher magnification SEM image [Fig. 1(b)–1(d)] are from the rectangle-enclosed area of (B), (C), and (D) regions in Fig. 1(a), respectively, showing that the nanotips have smaller diameters in the top region than the bottom region, giving rise to a much higher aspect ratio. The structure of the tungsten oxide nanotips was characterized with XRD, which is shown in Fig. 1(e). All of the diffraction peaks, except one peak from the silicon substrate, can be indexed to monoclinic structured $W_{18}O_{49}$ (JCPDs cards: 36–101).

The detailed microstructures of the tungsten oxide nanotips were characterized using TEM. Low magnification TEM images in Fig 2(a) and 2(b) show two kinds of typical tungsten oxide nanotips, respectively. The diameter of the nanotip in Fig 2(a) decreases slowly from bottom to top with a small slope. In contrast, the diameter of the nanotip in Fig. 2(b) decreases abruptly, and the diameter keeps uniform in each section, displaying a segment-by-segment laddered structure. In addition, Fig. 2(c) shows a tungsten oxide nanotip with a segmented tip-on-tip shape. Figure 2(d) is the enlarged TEM image from the rectangle-enclosed area of Fig. 2(c), showing that the diameter of the top tip is ~20 nm. The corresponding selected area electron diffraction (SAED) pattern [inset of Fig. 2(d)] shows that the entire nanotip is single crystalline with a growth direction of [010]. Figure 2(e) is the high-resolution TEM image of the same tungsten oxide nanotip. Two sets of space fringes of 0.38 and 0.46 nm are indexes to (010) and ($\bar{1}$03), respectively.

No catalyst was used in our growth process. In addition, the SEM and TEM study shows no nanoparticles at the ends of tungsten oxide nanotips. Accordingly, the vapor-liquid-solid (VLS)[23] growth process cannot be applied to the growth of our tungsten oxide nanotips. The vapor-solid (VS)[24] growth process may be suitable for our case. During the heating process, tungsten oxide might be formed on the surface of the tungsten powders; the oxide was evaporated and redeposited on the substrate surface, forming one-dimensional nanostructures. Alternatively, the tungsten metal was vaporized first; a subsequent oxidation during the deposition on the substrate may also form the nanostructure. The formation of the segmented tip-shape structure may be dominated by the temperature change in the growth process, which will thus change the supersaturation, substrate tem-
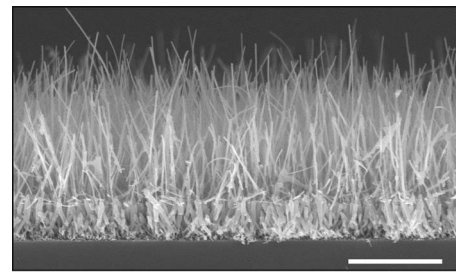

FIG. 3. SEM image of quasialigned WO_3 nanotips arrays. Scale bar 5 μm.

perature, and temperature gradient. Using the two-step growth process with different temperature parameter and further oxidation, well-separated WO_3 nanotips arrays have also been formed, as shown in Fig. 3.

The field-emission measurements were carried out with a transparent anode technique[8] in a chamber having vacuum of ~2.0×10^{-7} Torr. CCD camera was used to record emission site distributions. A typical series of spatial distribution of emission sites and their variation with applied gap field (3.9, 4.3, and 4.5 MV/m) were recorded, as shown in Figs. 4(b)–4(d) respectively. With increasing field, the emission became stronger, resulting in an increased number of bright spots. A comparison between the CCD camera image of the sample [Fig. 3(a)] and the emission site distribution images shows that the distribution in the emission site is very uniform. Also, their intensity is quite homogeneous.

A typical plot of emission current versus electric field ($J-E$) for our tungsten oxide nanotips arrays measured at a vacuum gap of 200 μm is shown in Fig. 5(a). After a few cycles of applying the gap field, the emission seemed to reach a stable stage. The electron field-emission turn-on field (E_{to}) and threshold field (E_{thr}), defined as the macroscopic field required to produce a current density of 10 μA/cm^2 and 10 mA/cm^2, are about 2.0 and 4.37 MV/m, respectively. Reproducibility tests from 12 different samples indicate that most of the tungsten oxide nanotips arrays have E_{thr} in the range of 4.5±0.7 MV/m. The performance of field emission from the as-synthesized tungsten oxide nanotip was better than that of the reported for $W_{18}O_{49}$ nanowires/nanotubes.[20] The reasons may be as the follows. First, our nanotips with a needle shape have a higher aspect ratio; second, the nanotips are well separated from each other, which will decrease the screen effect and increase the
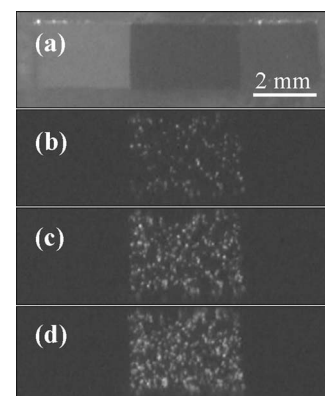

FIG. 4. (a) CCD camera image of the sample. The spatial distribution of emitting sites of tungsten oxide nanotip arrays with variation applied gap field: (b) E=3.9 MV/m, (c) E=4.3 MV/m, (d) E=4.5 MV/m. The dotted line in (a) indicates the boundary of the sample.
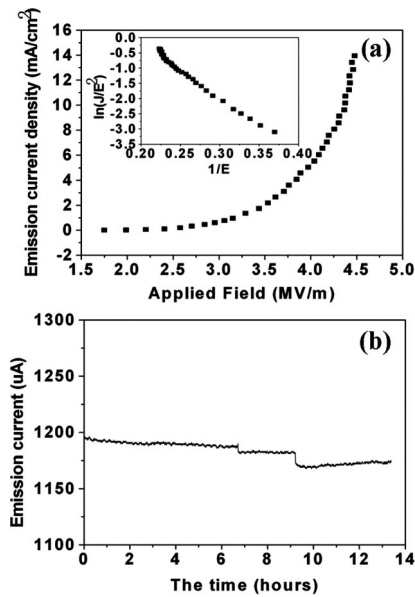
FIG. 5. (a) Field-emission current density versus electric field (*J-E*) plot of tungsten oxide nanotip arrays. The inset is the corresponding F–N plot. (b) The field-emission current stability of the tungsten oxide nanotip arrays over time.

field enhancement factor as well. It is interesting to find that the corresponding Fowler–Nordheim (F-N) plot [inset in Fig. 5(a)] exhibits nonlinearity. The slope at the high-field region is larger than that in the low-field region. This phenomenon could be explained by the varied field enhancement factor due to the different tip shape.[8,25] Our observation with SEM [Fig. 1(a)] shows that the nanotips have various lengths and radii. Therefore, the field enhancements for these nanotips were different, which would result in different turn-on fields. This explanation is also consistent to the result of emission site observation [Fig. 3(a), 3(b), and 3(d)], i.e., more and more emission sites were shown at a high field. The emission stability of tungsten oxide nanotips was examined at a fixed voltage (dc mode) through automatic recording of the emission current every second. Figure 5(b) shows the stability during 13.5 h of continuous operation at a current of about 1200 μA, the degradation was observed to be ~2.0%.

In summary, quasialigned tungsten oxide nanotip arrays have been grown with the two-step growth method. This method may be suitable for the growth of other materials nanotip arrays. Stable and uniform field emission with a low threshold field was observed from the tungsten oxide nanotip arrays. These findings indicate that tungsten oxide nanotip arrays have a potential application in field emission and flat panel display.

[1]C. A. Spindt, I. Brodie, L. Humphrey, and E. R. Westerberg, J. Appl. Phys. **47**, 5248 (1976).
[2]W. B. Choi, D. S. Chng, J. H. Kang, H. Y. Kim, Y. W. Jin, I. T. Han, Y. H. Lee, J. E. Jung, N. S. Lee, G. S. Park, and J. M. Kim, Appl. Phys. Lett. **75**, 3129 (1999).
[3]W. A. de Heer, A. Chatelain, and D. Ugarte, Science **269**, 1179 (1995).
[4]S. S. Fan, M. G. Chapline, N. R. Franklin, T. W. Tombler, A. M. Cassell, and H. J. Dai, Science **283**, 512 (1998).
[5]V. N. Tondare, C. Balasubramanian, S. V. Shende, D. S. Joag, V. P. Godbole, S. V. Bhorakar, and M. Bhadbhade, Appl. Phys. Lett. **80**, 4813 (2002).
[6]Z. L. Wang, R. P. Gao, W. A. de Heer, and P. Poncharal, Appl. Phys. Lett. **80**, 856 (2002).
[7]Z. S. Wu, S. Z. Deng, N. S. Xu, J. Chen, J. Zhou, and J. Chen, Appl. Phys. Lett. **80**, 3829 (2002).
[8]J. Chen, S. Z. Deng, N. S. Xu, S. H. Wang, X. G. Wen, S. H. Yang, C. L. Yang, J. N. Wang, and W. K. Ge, Appl. Phys. Lett. **80**, 3620 (2002).
[9]J. Zhou, N. S. Xu, S. Z. Deng, J. Chen, J. C. She, and Z. L. Wang, Adv. Mater. (Weinheim, Ger.) **15**, 1835 (2003).
[10]B. Xiang, Q. X. Wang, Z. Wang, X. Z. Zhang, L. Q. Liu, J. Xu, and D. P. Yu, Appl. Phys. Lett. **86**, 243103 (2005).
[11]Z. W. Pan, H. L. Lai, F. C. K. Au, X. F. Duan, W. Y. Zhou, W. S. Shi, N. Wang, C. S. Lee, N. B. Wong, S. T. Lee, and S. S. Xie, Adv. Mater. (Weinheim, Ger.) **12**, 1186 (2000).
[12]Y. B. Li, Y. Bando, D. Golberg, and K. Kurashima, Appl. Phys. Lett. **81**, 5048 (2002).
[13]J. Chen, S. Z. Deng, N. S. Xu, W. X. Zhang, X. G. Wen, and S. H. Yang, Appl. Phys. Lett. **83**, 746 (2003).
[14]Y. B. Li, Y. Bando, and D. Golberg, Appl. Phys. Lett. **84**, 3603 (2004).
[15]Q. Zhao, J. Xu, X. Y. Xu, Z. Wang, and D. P. Yu, Appl. Phys. Lett. **85**, 5331 (2004).
[16]L. Vila, P. Vincent, L. D. D. Pra, G. Pirio, E. Minoux, L. Gangloff, S. D. Champagne, N. Sarazin, E. Ferain, R. Leger, L. Piraux, and P. Legagneux, Nano Lett. **4**, 521 (2004).
[17]C. Santato, M. Odziemkowski, M. Ulmann, and J. Augustynski, J. Am. Chem. Soc. **123**, 10639 (2001).
[18]J. L. Solis, S. Saukko, L. Kish, C. G. Granqvist, and V. Lantto, Thin Solid Films **391**, 255 (2001).
[19]K. Sayama, K. Mukasa, R. Abe, Y. Abe, and H. Arakawa, Chem. Commun. (Cambridge) **23**, 2416 (2001).
[20]Y. B. Li, Y. Bando, and D. Golberg, Adv. Mater. (Weinheim, Ger.) **15**, 1294 (2003).
[21]J. G. Liu, Z. J. Zhang, Y. Zhao, X. Su, S. Liu, and E. G. Wang, Small **1**, 310 (2005).
[22]J. Zhou, Y. Ding, S. Z. Deng, L. Gong, N. S. Xu, and Z. L. Wang, Adv. Mater. (Weinheim, Ger.) **17**, 2107 (2005).
[23]A. M. Morales, and C. M. Lieber, Science **279**, 208 (1998).
[24]W. Z. Pan, Z. R. Dai, and Z. L. Wang, Science **291**, 1947 (2001).
[25]J. Chen, S. Z. Deng, J. C. She, N. S. Xu, W. X. Zhang, X. G. Wen, and S. H. Yang, J. Appl. Phys. **93**, 1744 (2003).